

miR-93-5p-Containing Exosomes Treatment Attenuates Acute Myocardial Infarction-Induced Myocardial Damage

Jiwen Liu,^{1,5} Mei Jiang,^{2,5} Shengqiong Deng,^{3,5} Jide Lu,¹ Hui Huang,¹ Yu Zhang,¹ Peihua Gong,¹ Xumin Shen,¹ Huanjun Ruan,¹ Mingming Jin,⁴ and Hairong Wang¹

¹Department of Cardiology, Shanghai Gongli Hospital, The Second Military Medical University, Shanghai 200135, China; ²Department of Neurology, Shanghai Gongli Hospital, The Second Military Medical University, Shanghai 200135, China; ³Department of Clinical Laboratory, Shanghai Gongli Hospital, The Second Military Medical University, Shanghai 200135, China; ⁴Department of Central Laboratory, Shanghai Gongli Hospital, The Second Military Medical University, Shanghai 200135, China

Adipose-derived stromal cells (ADSCs) have been considered as an attractive therapeutic tool. Accumulating evidence indicates that the healing effects of ADSCs are mainly related to paracrine action rather than transdifferentiation. Data show that the expression of miR-93-5p has a cardio-protective effect after acute myocardial infarction (AMI). To identify whether miR-93-5p-encapsulating exosomes that form ADSCs have a better cardio-protective effect, we investigated the inflammatory factors and miR-30d-5p expression in clinical levels. A rat model of AMI and an *in vitro* model of hypoxic H9c2 cells were established to study the protective mechanism of miR-93-5p in ischemia-induced cardiac injury. The results show that the expression of inflammatory cytokines and miR-93-5p were increased following AMI in both patients and animal models. Moreover, treatment with ADSC-derived miR-93-5p-containing exosomes has a greater protective effect on infarction-induced myocardial damage than simple exosome processing. Furthermore, *in vitro* experiments confirmed that the expression of miR-93-5p can significantly suppress hypoxia-induced autophagy and inflammatory cytokine expression by targeting Atg7 and Toll-like receptor 4 (TLR4), respectively, and was confirmed with Atg7 or TLR4 overexpression. The results also show that autophagy activation can promote inflammatory cytokine expression indirectly. Taken together, these results suggest that the miR-93-5p-enhanced ADSC-derived exosomes prevent cardiac injury by inhibiting autophagy and the inflammatory response.

INTRODUCTION

Acute myocardial infarction (AMI) is one of the most serious cardiovascular diseases.¹ An early and accurate diagnosis can guarantee immediate initiation of reperfusion therapy to potentially reduce the mortality rate. Recently, many attempts have been made to improve the outcome of AMI using stem cells in preclinical and clinical studies.²⁻⁵ Among the various sources of stem cells, mesenchymal stem cells (MSCs), particularly adipose-derived MSCs, have been used to treat AMI.^{6,7} The earliest preclinical studies suggested

that MSCs have the potential to differentiate into multiple cardiac cell types including cardiomyocytes, vascular endothelial cells, and vascular smooth muscle cells.^{2,7,8} However, subsequent studies were not able to reproduce this remarkable differentiation capacity of MSCs. Rather, it was reported that most intravenously injected cells are trapped in the lung rather than engrafted in the heart.^{9,10} Even when MSCs are administered to a swine heart via the coronary artery following AMI induction, only 6% of the injected cells remained in the infarct zones 14 days after AMI induction.⁹ Furthermore, the supernatant of MSC cultures reportedly improves cardiac function.^{9,11,12} These results suggest that MSCs improve cardiac function via the secretion of paracrine factors rather than via direct differentiation of MSCs into cardiac cell types. Furthermore, MSC transplantation entails several problems such as low survival rate and stem cell tumorigenesis.¹³ Consequently, we suspect that secreted paracrine factors from MSCs may play an important role in the repair and regeneration of cardiac tissues.

Exosomes are a type of secreted vesicle (also referred to as extracellular vesicles or EVs) that are 30–100 nm in diameter and contain a variety of biologically active molecules, such as proteins, mRNAs, and microRNAs (miRNAs).¹⁴ miRNAs are short non-coding RNAs that regulate gene expression post-transcriptionally through translational repression or mRNA degradation, and play roles in the pathogenesis of various human diseases including chronic AMI.^{15,16} One study showed that miR-93 elevation has a cardio-protective effect

Received 30 November 2017; accepted 24 January 2018;
<https://doi.org/10.1016/j.omtn.2018.01.010>

⁵These authors contributed equally to this work.

Correspondence: Hairong Wang, Department of Cardiology, Shanghai Gongli Hospital, Second Military Medical University, 219 Miao-Pu Road, Shanghai 200135, China.

E-mail: hairong19@yahoo.com

Correspondence: Mingming Jin, Department of Central Laboratory, Shanghai Gongli Hospital, Second Military Medical University, 219 Miao-Pu Road, Shanghai 200135, China.

E-mail: asdjinmingming@126.com



Table 1. Demographic Characteristics of AMI Cases and Controls

Characteristics	AMI Cases (n = 60)	Controls (n = 30)	p Value
Age, mean \pm SD (years)	63.58 \pm 13.45	61.55 \pm 11.24	0.161
Gender, n (%)			
Men	32 (53.3)	17 (56.7)	0.113
Women	28 (46.7)	13 (43.3)	0.123
Diabetes, n (%)	12 (20.0)	6 (20.0)	0.773
Current smoker, n (%)	24 (40.0)	11 (36.7)	0.329
Current drinker, n (%)	15 (25.0)	7 (23.3)	0.198
Hypertension, n (%)	31 (51.7)	6 (20.0)	0.168
TC, mean \pm SD (mg/dL)	4.29 \pm 1.03	4.01 \pm 0.84	0.101
BG on admission, mean \pm SD (mg/dL)	6.44 \pm 2.28	5.24 \pm 1.32	0.004
BNP, mean \pm SD (pg/mL)	2,036.24 \pm 659.33	628.39 \pm 543.56	0.024
Serum triglycerides, mean \pm SD (mmol/L)	1.59 \pm 1.02	1.39 \pm 0.63	0.009
Serum HDL cholesterol, mean \pm SD (mmol/L)	0.98 \pm 0.22	1.11 \pm 0.36	0.512
Serum LDL cholesterol, mean \pm SD (mmol/L)	2.99 \pm 0.88	2.61 \pm 0.71	0.198

p < 0.05 means that the difference between two groups is significant. AMI, acute myocardial infarction; BG, blood glucose; BNP, brain natriuretic peptide; HDL, high-density lipoprotein; LDL, low-density lipoprotein; TC, total cholesterol.

after MI,¹⁷ but the specific regulatory mechanism is not clear. A number of studies have demonstrated that miRNA-mediated autophagy and modulation of inflammation play an important part in disease progression.^{18–20} Bioinformatics analysis (<http://www.targetscan.org/>) found that miR-93-5p targets Toll-like receptor 4 (TLR4) and Atg7, suggesting that the expression of miR-93-5p plays an important role in the regulation of autophagy and inflammation.

Autophagy and the inflammatory response can be activated after AMI.^{21–23} Autophagy is a homeostatic process that can prevent damage to healthy cells. However, sustained autophagy can lead to cell death in an emergency situation. Increasing evidence shows that there are potential interactions between autophagy and inflammation. It has been reported that inflammation can be inhibited via enhancement of autophagy.²⁴ In contrast, other data show that suppression of autophagy can attenuate inflammation.²⁵ Thus, we predicted that the protective effect of miR-93-5p on the heart after AMI may be due to regulation of autophagy and the inflammatory response.

To elucidate the potential role of miR-93-5p in the therapeutic effect of adipose-derived stromal cell (ADSC)-derived exosomes, we investigated the expression of miR-93-5p after AMI both in patients and in animal models. We analyzed the target genes of miR-93-5p and the relationship among miR-93-5p, apoptosis, inflammation, and autophagy both *in vivo* and *in vitro*. These data may provide new evidence that exosomes derived from miR-93-5p-overexpressing ADSCs have better therapeutic effects on AMI.

RESULTS

The Expression of Both miR-93-5p and Inflammatory Factor in Serum Was Increased in AMI Patients

Previous study found that the expression miR-93 is elevated both in ventricle tissue and blood in a mouse MI model, and miR-93 is secreted from cardiomyocytes cultured under hypoxia. The results also show that the expression of miR-93 inhibits apoptosis and protects cardiomyocytes from ischemia/reperfusion injury.¹⁷ To identify whether the expression of miR-93 increased after AMI and to shed light on the related mechanism, we collected serum from 60 AMI patients and 30 healthy controls. The data demonstrated that AMI did not alter serum levels of total cholesterol (TC), brain natriuretic peptide (BNP), high-density lipoprotein (HDL) cholesterol, or low-density lipoprotein (LDL) cholesterol, but did increase blood glucose (BG), BNP, and serum triglycerides (Table 1). RT-PCR analyses found that, compared with the control group, the expression of miR-93-5p in serum was significantly increased after AMI (Figure 1A). ELISA detection also showed that the inflammatory factors interleukin-6 (IL-6), IL-1 β , and tumor necrosis factor alpha (TNF- α) were all significantly increased in the serum of AMI patients (Figures 1B–1D).

Treatment with ADSC-Derived miR-93-5p-Containing Exosomes Can Significantly Attenuate Myocardial Damage after AMI

Increasing evidence shows that exosomes from ADSCs have therapeutic effects on different diseases, including liver fibrosis, erectile dysfunction, and ischemia/reperfusion injury.^{26–28} Primary ADSCs from Sprague-Dawley rats were isolated, and ADSCs with a typical cobblestone-like morphology were obtained to identify whether exosomes from ADSCs have a protective effect on myocardial cells after AMI (Figure 2A). The result also showed that isolated ADSCs were positive for the MSC markers CD29, CD90, CD44, and CD105, and negative for the endothelial markers CD34 and von Willebrand factor (vWF) (Figures 2B–2H). Exosomes were then purified from ADSCs, and transmission electron microscopy was used to identify exosomes from the ADSC culture medium. Ultrastructural analysis of ADSC-derived exosomes revealed they had a diameter of around 100 nm (Figure 3A), while the size distribution was determined to be slightly below 100 nm by dynamic light scattering (Figure 3B). The expression of the exosome markers CD9, CD63, and TSG101 was then confirmed by western blotting (Figure 3C).

To identify whether the expression of miR-93-5p is responsible for the protective effect of exosomes on myocardial cells after AMI, we transfected ADSCs with miR-93-5p overexpression mimic and cultured them for 48 hr, then harvested for RT-PCR detection. The results showed that the expression of miR-93-5p in exosomes was increased after transfection with miR-93-5p mimic (Figure 3D).

To assess the role of miR-93-5p-containing exosomes in myocardial injury in a rat model, we harvested serum for ELISA and used myocardial tissue for immunohistochemical analysis 4 weeks after

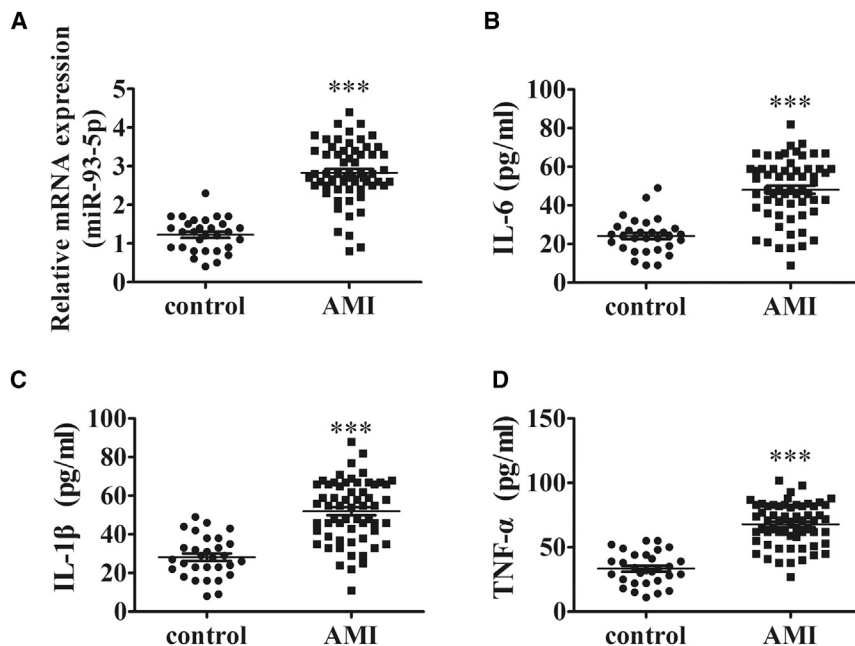


Figure 1. miR-93-5p and Inflammatory Factors Expression in AMI Patients

(A) RT-PCR analyses of miR-93-5p expression in the serum of AMI patients. The results show that expression of miR-93-5p in AMI patients was significantly increased compared with controls. Data are presented as means \pm SD. (B–D) ELISA shows the expression of the inflammatory factors IL-6 (B), IL-1 β (C), and TNF- α (D) in the serum of AMI patients. Data are presented as means \pm SD. ***p < 0.001 versus control.

coronary artery ligation. Infarct volume was measured using 2,3,5-triphenyl-tetrazolium-chloride (TTC) (Figure 4A) and H&E (Figure 4B) staining, respectively. The results showed that infarct volume was significantly increased after AMI, but exosome treatment significantly decreased infarct volume and treatment with miR-93-5p-containing exosomes was especially effective (Figure 4C). Terminal deoxynucleotidyl transferase-mediated dUTP-biotin nick end labeling (TUNEL) showed that treatment with miR-93-5p-containing exosomes exerted a stronger suppressive effect on ischemia-induced myocardial apoptosis (Figures 4D and 4E).

Treatment with ADSC-Derived miR-93-5p-Containing Exosomes Significantly Suppressed Autophagy and Inflammation after AMI

To identify whether the protective effect of miR-93-5p-containing exosomes is related to autophagy and inflammation, we collected myocardial tissue samples for western blot analysis. The results showed that autophagy increased after AMI. Treatment with miR-93-5p-containing exosomes had a greater effect than simple exosomes in mediating autophagy inhibition. Western blot detection shows that miR-93-5p-containing exosomes have more effect on suppressed P62 expression, but increased LC3-II/I and Atg7 levels in myocardial tissue (Figures 5A–5D). Further results showed that the TLR4/NF- κ B (nuclear factor- κ B) signal pathway was involved in AMI-induced myocardial damage regulation. miR-93-5p-containing exosome treatment significantly suppressed infarction-induced TLR4 expression and NF- κ B p65 phosphorylation (Figures 5E–5G). ELISA showed that expression of the inflammatory factors IL-6, IL-1 β , and TNF- α in serum of AMI patients was decreased after treatment with exosomes, especially with miR-93-5p-containing exosomes (Figures 5H–5J).

miR-93-5p Expression in H9c2 Cells Inhibited Hypoxia-Induced Myocardial Cell Injury by Suppressing Atg7-Mediated Autophagy

To investigate the protective effect of miR-93-5p on hypoxia-induced myocardial cell injury and Atg7-mediated autophagy, we constructed miR-93-5p-overexpressing H9c2 cells (Figure 6A). To further identify the effect of Atg7 expression in autophagy, we constructed an Atg7 overexpression vector and transfected it into H9c2 cells for 48 hr before detection by western blot (Figure 6B) and RT-PCR (Figure 6C). The results showed that after transfection with the Atg7 overexpression vector, the expression level of Atg7 in H9c2 cells increased at both the protein and the mRNA level. Then H9c2 cells were exposed to hypoxic conditions for up to 24 hr to simulate a hypoxic environment. Apoptosis of H9c2 cells was assessed using flow cytometry with annexin V (AV)-fluorescein isothiocyanate (FITC) staining. The results showed that the apoptosis rate of H9c2 cells was significantly increased after exposure to hypoxic conditions. miR-93-5p overexpression significantly suppressed hypoxia-induced apoptosis, but Atg7 overexpression reversed the protective effect of miR-93-5p. These data suggest that miR-93-5p can target the 3' UTR of Atg7 at the mRNA level, but cannot reduce the transfected Atg7 mRNA because the transfected Atg7 overexpression vector does not transcribe the 3' UTR of the mRNA of Atg7 (Figures 6D and 6E). Immunofluorescence analysis showed that hypoxia treatment significantly promoted the generation of autophagy plaques in H9c2 cells, but this was inhibited by miR-93-5p overexpression. Meanwhile, Atg7 overexpression reversed this inhibitory effect of miR-93-5p (Figures 6F and 6G). LC3 and P62 expression in H9c2 cells were measured with western blotting. The result also showed that miR-93-5p overexpression inhibited hypoxia-induced expression of LC3 and inhibition of P62 expression. Atg7 overexpression reversed the inhibitory effect of miR-93-5p (Figures 6H–6J).

miR-93-5p Expression in H9c2 Cells Inhibited Hypoxia-Induced Myocardial Cell Injury by Suppressing the TLR4/NF- κ B-Mediated Inflammatory Response

A TLR4 overexpression vector was constructed and transfected into H9c2 cells for 48 hr before detection by western blot (Figure 7A) and RT-PCR (Figure 7B) to analyze the protective effect of

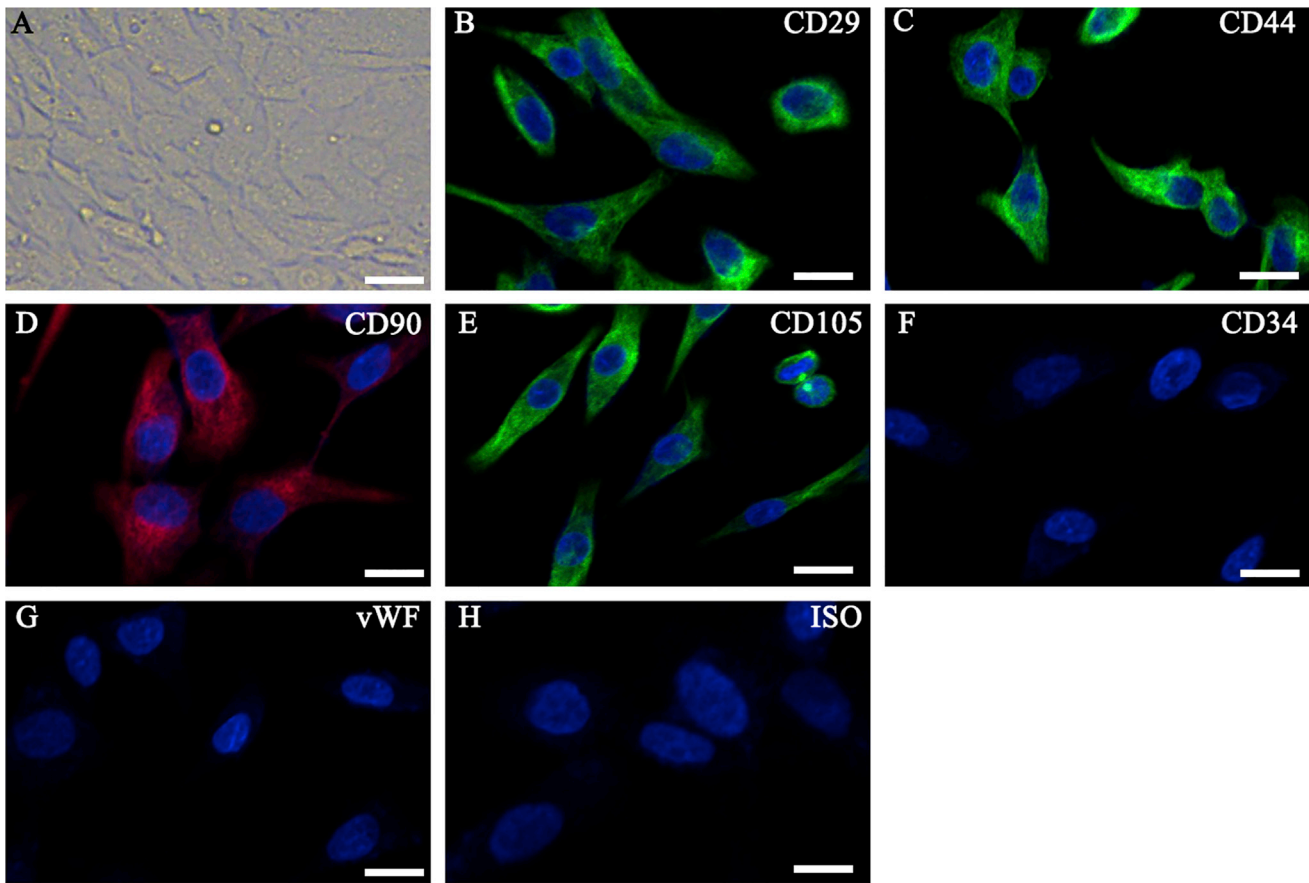


Figure 2. Characteristics of Adipose-Derived Stem Cells

(A) Typical cobblestone-like morphology. (B–H) Determination of cell surface markers by immunofluorescence staining. The antibodies were labeled with either fluorescein isothiocyanate (FITC; green color) or phycoerythrin (PE; red color). The results showed positive staining for CD29 (B), CD44 (C), CD90 (D), and CD105 (E) and negative staining for CD34 (F) and von Willebrand factor (vWF) (G). Negative IgG isotype controls (H) are shown. Scale bars, 20 μ m.

miR-93-5p in hypoxia-induced myocardial cell injury and TLR4/NF- κ B-mediated inflammation. The results showed that after transfection with the TLR4 overexpression vector, TLR4 expression in H9c2 cells was increased at both the protein and the mRNA level. Then H9c2 cells were exposed to hypoxic conditions for up to 24 hr to simulate a hypoxic environment. Apoptosis of H9c2 cells was assessed using flow cytometry with AV-FITC staining. The results showed that miR-93-5p overexpression significantly suppressed hypoxia-induced apoptosis, but that TLR4 overexpression reversed the protective effect of miR-93-5p (Figures 7C and 7D). Western blotting showed that miR-93-5p overexpression suppressed hypoxia-induced phosphorylation of NF- κ B p65, but TLR4 overexpression reversed the inhibitory effect of miR-93-5p (Figures 7E and 7F). ELISA also showed that miR-93-5p overexpression suppressed hypoxia-induced IL-6, IL-1 β , and TNF- α expression, but this effect was reversed by TLR4 overexpression (Figures 7G–7I).

Both Atg7 and TLR4 Are Direct Targets of miR-93-5p

To identify possible interactions between miR-93-5p and Atg7 or TLR4, we used bioinformatics analysis to predict possible targets

(<http://www.targetscan.org/>). Overlap analyses showed that miR-93-5p had a broadly conserved binding site with Atg7 (Figure 8A). A mutated version of the Atg7 3' UTR was constructed in which five complementary nucleotides in the binding site were altered. This mutated construct was fused to the luciferase coding region (PYr-Atg7 3' UTR) and co-transfected into HEK293T cells along with miR-93-5p mimic. The relative luciferase activity showed that when the wild-type Atg7 3' UTR was co-transfected with the miR-93-5p mimic, Atg7 expression was significantly decreased compared with co-transfection with the control miRNA. However, this effect was not observed after transfection of the mutant 3' UTR of Atg7, indicating that miR-93-5p can specifically target and suppress the 3' UTR of Atg7 (Figure 8B). Western blotting (Figure 8C) and RT-PCR (Figure 8D) analyses further confirmed that miR-93-5p overexpression significantly inhibited Atg7 expression at both the protein and the mRNA level *in vitro*. These data suggest that miR-93-5p-abundant Exos have a greater effect in suppressing autophagy. Further study also identified that miR-93-5p can specifically target and suppress the 3' UTR of TLR4 (Figures 8E–8H).

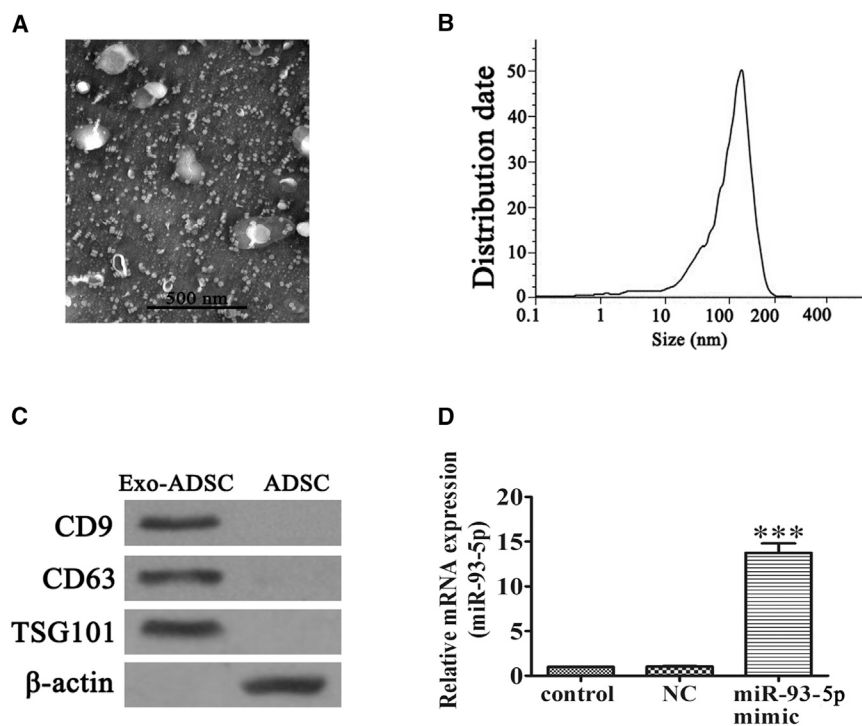


Figure 3. Exosome Characterization

(A) Electron microscopic image of exosomes. (B) Results of nanoparticle tracking analysis of exosomes. Scale bars, 500 nm. (C) Western blots using TSG101, CD9, and CD63 as markers of exosomes from ADSCs. (D) RT-PCR shows miR-93-5p expression in exosomes from ADSCs after transfection with miR-93-5p mimic for 48 hr. The data are presented as mean \pm SD (n = 3). ***p < 0.001 versus control group.

confirmed by a bifluorescein reporter experiment, suggesting that the protective effect of miR-93-5p is associated with autophagy inhibition.

Our bioinformatics analysis also found that miR-93-5p expression results in targeting the 3' UTR of TLR4, which plays an important role in mediating the inflammatory response during hypoxia or under ischemic conditions.^{40,41} There is increasing evidence that downregulation of TLR4 expression can significantly suppress ischemia-induced cardiomyocyte apoptosis after AMI.⁴² Our *in vitro* experi-

ments also showed that miR-93-5p suppressed hypoxia-induced apoptosis and inflammatory factor expression by targeting TLR4, which was confirmed by bifluorescein reporter experiments. These data suggest that the protective effect of miR-93-5p is associated with TLR4 inhibition.

In summary, our study found that miR-93-5p-containing exosomes have a greater protective effect on AMI-induced myocardial damage. For the first time, our *in vitro* and *in vivo* results confirmed that exosomal miR-93-5p prevents myocardial injury by targeting Atg7-mediated autophagy and TLR4-mediated inflammatory responses. These results provide novel insights into the molecular and therapeutic mechanism of why ADSC-derived miR-93-5p-containing exosomes can attenuate myocardial damage.

MATERIALS AND METHODS

Patients and Clinical Characteristics

Sixty AMI patients (28 females and 32 males; average age 63.58 ± 13.45 years) were recruited between May 1, 2017, and October 31, 2017, at the Pudong New Area Gongli Hospital, Shanghai, China. All patients were diagnosed as having AMI according to the electronic computerized hospitalization records. Age- and sex-matched healthy individuals were also selected from the Pudong New Area Gongli Hospital (17 males and 13 females; average age 61.55 ± 11.24 years). Twelve patients had a history of diabetes. Thirty-one patients were diagnosed with hypertension, whereas 24 and 15 patients had histories of smoking and drinking alcohol, respectively. All serum samples were frozen in liquid nitrogen immediately after taken from the cubital vein within 24 hr of symptom onset and were used for further analysis.

DISCUSSION

Ischemic heart disease is the leading cause of human mortality and morbidity in the world, underscoring the need for innovative new therapies.²⁹ Exosomes are small nanometer-sized vesicles of endocytic origin. They essentially function as intercellular shuttles loaded with a cargo of protein and RNA by effector cells for off-loading in target cells.^{30–32} Accumulating evidence has shown that exosomes from MSCs play a role in their therapeutic effect in many diseases including AMI.^{33–35} Follow-up studies have confirmed that MSC-derived exosomes can be used as a vehicle for delivery of therapeutic miRNA.^{36,37}

In the present study, we report that the levels of circulating miR-93-5p in human AMI are increased in comparison with healthy adults. To identify whether miR-93-5p has a therapeutic effect in AMI, we constructed an AMI model using Sprague-Dawley rats. Our study revealed that miR-93-5p-modified ADSCs effectively packaged miR-93-5p into secreted exosomes, which delivered their miR-93-5p content into AMI rats, significantly suppressing infarction-induced myocardial damage by inhibiting autophagy and inflammation.

In this study, we observed increased expression of autophagy markers in myocardial tissues after AMI. The function of autophagy is to ensure the delivery of metabolic substrates to cells so as to fulfill their energy demand during stress especially in an inflammatory environment, thus supporting cell survival.^{38,39} However, hyperactivation of autophagy will result in cell death designated as “autophagic cell death.” Our *in vitro* experiments show that miR-93-5p suppressed hypoxia-induced autophagy by targeting Atg7, and this was

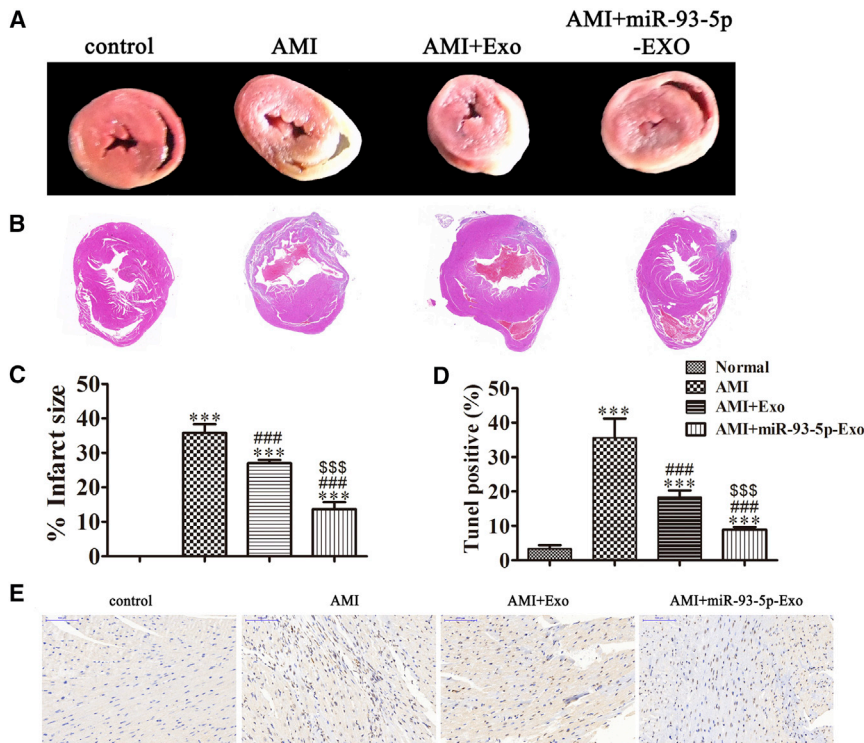


Figure 4. miR-93-5p Abundant Exosomes Have a Greater Protective Effect on Suppressing AMI-Induced Myocardial Damage

(A) Photographs showing representative TTC staining 30 days after acute myocardial infarction treatment with or without exosomes. The slices were incubated with 2,3,5-triphenyl-tetrazolium-chloride (TTC) for 10 min. Non-infarcted myocardium, which contained dehydrogenase, was stained brick red by reacting with TTC, whereas necrotic (infarcted) tissue was unstained because of the lack of enzyme. (B) H&E staining of heart sections 30 days after myocardial infarction. (C) The infarct size was measured and calculated as a percentage of the total area. The data are presented as mean \pm SD (n = 3). (D) The myocardial apoptosis of infarction areas was measured by TUNEL. Scale bars, 100 μ m. (E) The relative percentages of apoptotic cells were calculated. The data are presented as mean \pm SD (n = 3). ***p < 0.001 versus control group; ###p < 0.001 versus AMI group; \$\$\$p < 0.001 versus exosome group.

culture medium was added. The medium was changed every 3 days. Cells were passaged when they were \sim 90% confluent and were used at passage three. To confirm the identity of the cells, we incubated ADSCs with conjugated monoclonal antibodies against CD29,

The study was approved by the ethics committee of the Pudong New Area Gongli Hospital. All participants or their relatives were informed of the study and signed the consent forms before inclusion in the study.

Animals and Ethics Statement

Male Sprague-Dawley rats (180–230 g) were purchased from Shanghai Sippr Bk Laboratory Animals (Shanghai, China). All rats were allowed free access to food and water under controlled conditions (12/12 hr light/dark cycle with humidity of 60% \pm 5% and a temperature of 22°C \pm 3°C). All animals were treated in accordance with the Guide for the Care and Use of Laboratory Animals, and all experiments were approved and performed according to the guidelines of the Ethics Committee of Pudong New Area Gongli Hospital, Shanghai, China. All surgical procedures were performed under anesthesia, and every effort was made to minimize suffering. Rats were anesthetized by intraperitoneal injection of sodium pentobarbital (30 mg/kg).

Preparation, Culture, and Identification of ADSCs

Isolation and culture of ADSCs were conducted as previously described.⁴³ In brief, male Sprague-Dawley rats (80–120 g) were euthanized and adipose tissue was obtained from the inguinal depots and washed with PBS to remove any residual blood. The tissues were cut into 1 \times 1 mm sized pieces and digested with collagenase I. After centrifugation at 4,000 \times g for 5 min, the cell pellet was suspended in DMEM containing 10% fetal bovine serum (FBS)/1% penicillin-streptomycin/2 mM L-glutamine and incubated in a humidified atmosphere with 5% CO₂ at 37°C for 48 hr. The medium containing non-adherent cells was then removed and fresh

CD90, CD45, CD105, or vWF and CD34. Isotype-identical antibodies served as controls (PharMingen, San Diego, CA, USA). For the analyses of CD29, CD90, CD45, CD105, vWF, and CD34, cells were further incubated with a biotinylated horse anti-mouse IgG (H1L) antibody and FITC-conjugated streptavidin (Caltag, San Francisco, CA, USA). After treatment, the cells were fixed in 1% paraformaldehyde. Quantitative analyses were performed with a FACSCalibur flow cytometer (BD Biosciences, San Jose, CA, USA) and FlowJo software (FlowJo, Ashland, OR, USA). The logarithmic fluorescence intensities were recorded for 10,000–20,000 cells per sample.

Isolation and Identification of Exosomes from Conditioned Medium

The miR-93-5p mimics and the negative control (NC) were synthesized by GenePharma (Shanghai, China) and transfected into the ADSCs to a final oligonucleotide concentration of 20 nmol/L. The transfections were introduced by Lipofectamine 3000 (Invitrogen Life Technologies, Carlsbad, CA, USA) according to the manufacturer's instructions. After transfection for 48 hr, ADSCs were collected for miR-93-5p expression identification. Successful transfection cells are used for subsequent experiments.

At 80%–90% confluence, ADSCs (control, NC, or miR-93-5p overexpression group) were rinsed with PBS and cultured in microvascular endothelial cell growth medium-2 (EGM-2MV) media deprived of FBS and then supplemented with 1 \times serum replacement solution (PeproTech, Rocky Hill, NJ, USA) for an additional 24 hr. ADSCs

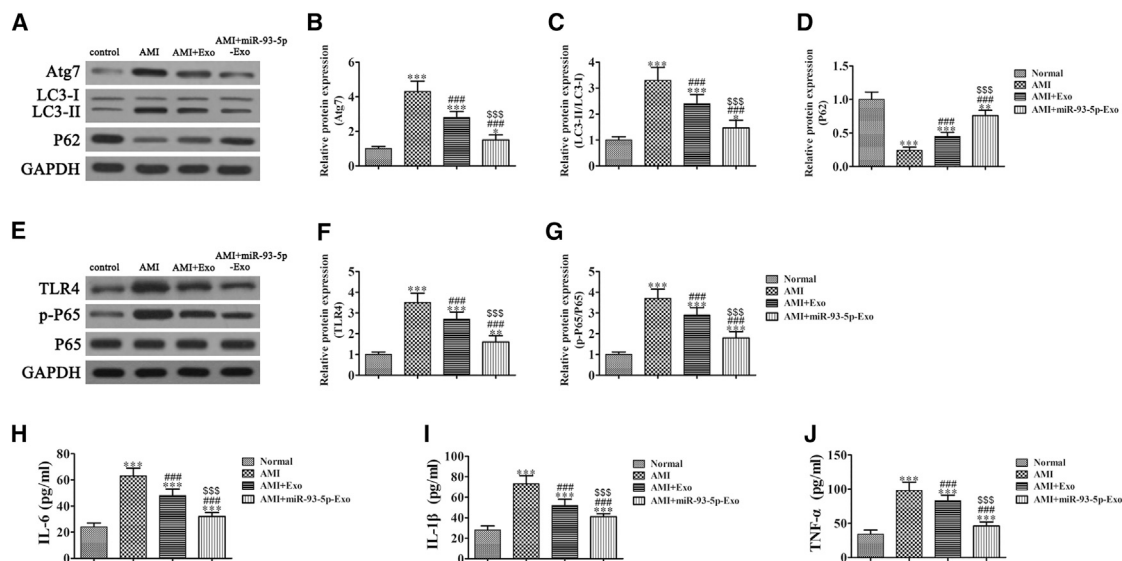


Figure 5. miR-93-5p-Exosome Treatment Suppressed Autophagy and the Inflammatory Response

(A) Western blot detection showed expression of the autophagy-related proteins Atg7, P62, and LC3. (B–D) Quantification of protein Atg7 (B), LC3 (C), and P62 (D) expression. The data are presented as means \pm SD. * $p < 0.05$; ** $p < 0.01$; *** $p < 0.001$ versus control; ### $p < 0.001$ versus AMI group; \$\$\$ $p < 0.001$ versus exosome group. (E) Western blot detection showing expression of TLR4 and NF- κ B p65. (F and G) Quantification of protein TLR4 (F) and NF κ B (G) expression. The data are presented as means \pm SD. ** $p < 0.01$; *** $p < 0.001$ versus control; ### $p < 0.001$ versus AMI group; \$\$\$ $p < 0.001$ versus exosome group. (H–J) ELISA showed the expression of the inflammatory factors IL-6 (H), IL-1 β (I), and TNF- α (J) in serum of AMI patients. Data are presented as means \pm SD. *** $p < 0.001$ versus control; ### $p < 0.001$ versus AMI group; \$\$\$ $p < 0.001$ versus exosome group.

in conditioned media were centrifuged at $300 \times g$ for 10 min and $2,000 \times g$ for 10 min to remove dead cells and cellular debris. Then approximately 10 mL of supernatant was mixed with 5 mL of ExoQuick-TC reagent (System Biosciences, Palo Alto, CA, USA) and incubated at 4°C for 12 hr. The ExoQuick/supernatant mixture was centrifuged at $1,500 \times g$ for 30 min to obtain a pellet containing exosomes, which was then resuspended in 250 μL of nuclease-free water. Total RNA and protein from exosomes were extracted using TRIzol-LS (Invitrogen, Carlsbad, CA, USA) and an Exosomal Protein Extraction kit (Invitrogen), following the manufacturer's instructions, respectively. Exosomes were stored at -80°C or used for downstream experiments. To determine the sizes of the purified vesicles, we performed nanoparticle tracking analysis (NTA) on a NanoSight LM10 (Malvern Instruments, Malvern, UK), and results were analyzed with NTA 3.0 software (Malvern Instruments).

The protein levels of CD63, CD9, and TSG101 (representative markers of exosomes) were detected with western blotting. The concentration of exosome proteins was assessed using a bicinchoninic acid assay kit (Beyotime, Suzhou, China). The ultrastructure of the exosomes was analyzed using a Libra 120 transmission electron microscope (Zeiss, Oberkochen, Germany).

Cell Lines and Cell Culture

The cardiomyoblast cell line H9c2 was purchased from the American Type Culture Collection (ATCC, Manassas, VA, USA) and cultured in DMEM supplemented with 10% FBS. To investigate whether

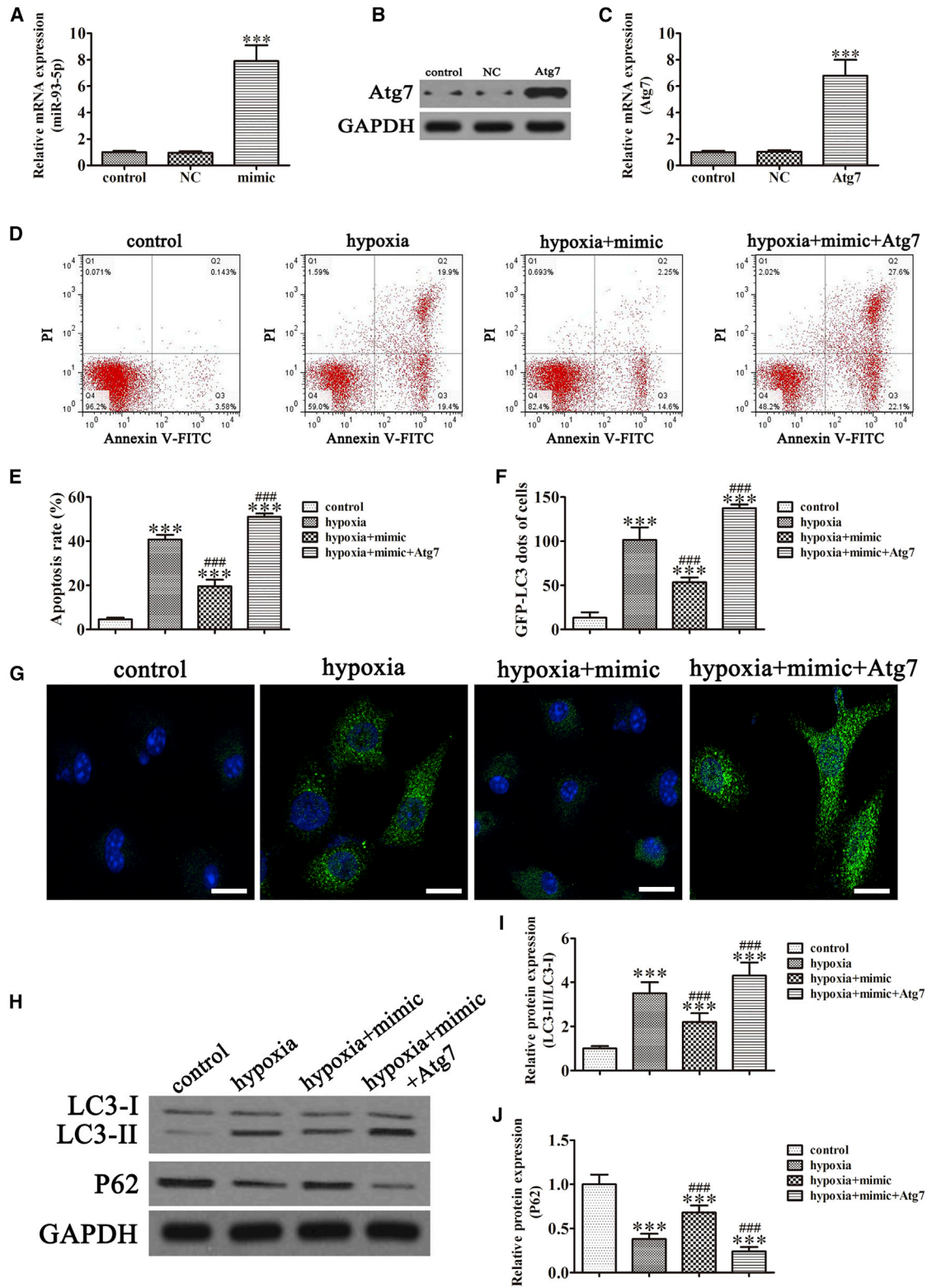
miR-93-5p plays an important role in exosome-mediated myocardial protection and to clarify its mechanism, we transfected H9c2 cells with the miR-93-5p mimic, TLR4, or Atg7 overexpression vector for 48 hr before exposure to hypoxia (93% N_2 , 2% O_2 , and 5% CO_2) for 24 hr. Then, the H9c2 cells were harvested for biological analyses.

Flow Cytometry

Flow cytometry was used to determine the rate of apoptosis of H9c2 cells. Apoptotic cells were differentiated from viable or necrotic cells by the combined application of AV-FITC and propidium iodide (PI). Cells were washed twice and adjusted to a concentration of 1×10^6 cells/mL with cold D-Hanks buffer. Then, AV-FITC (10 μL) and PI (10 μL) were added to 100 μL of cell suspension and incubated for 15 min at room temperature in the dark. Finally, 400 μL of binding buffer was added to each sample without washing and analyzed using flow cytometry. Each experiment was performed in triplicate.

mRNA Extraction and Real-Time PCR

RNA was isolated from serum, H9c2 cells, ADSCs, exosomes, or myocardial tissue using TRIzol (Invitrogen). cDNA was synthesized from 1 μg of total RNA, using oligo dT18 primers and SuperScript reverse transcriptase in a final volume of 21 μL . For standard PCR, 1 μL of the first-strand cDNA product was then used as a template for PCR amplification with Taq DNA polymerase (TaKaRa Bio, Shiga, Japan). PCR amplification was performed as follows: 30 thermocycles of 94°C for 30 s, 55°C for 30 s, and 72°C for 30 s, using oligo



(legend on next page)

nucleotides specific for miR-93-5p, TLR4, and ATG7 (Genechem, Shanghai, China). U6 small nuclear RNA was used as an internal reference for normalization.

Vector Construction and Transfection

For miR-93-5p overexpression, the miR-93-5p mimic or corresponding NC (miR-NC) was purchased from GenePharma (Shanghai, China). Human umbilical vein endothelial cells (HUVECs) were transfected with either the miR-93-5p mimic or miR-NC at a final concentration of 50 nM using Lipofectamine 2000 (Invitrogen) according to the manufacturer's protocol. The cells were then used for miR-93-5p expression analyses or for other experiments after 48 hr of transfection.

For the overexpression of TLR4 and Atg7, TLR4 and Atg7 cDNA with the 3' UTR were cloned into the pMSCV-hygro vector. The primers corresponded to the National Center for Biotechnology Information reference sequence and were as follows: TLR4 (forward, 5'-CAGAGCTCGGAGTACAAAACCTC-3' and reverse, 5'-GGTCTAGAAAAGTGCTTTTTCGAAG-3'); Atg7 (forward, 5'-CAGAGCTGTGCCTCATTGGGTC-3' and reverse, 5'-GGTCTAGACAGTAA TAAAGTGC-3'). The TLR4 or Atg7 cDNA was inserted into the pMD18-T Simple Vector (Takara, Otsu, Japan) to form the pMD18-T-TLR4 and pMD18-T-Atg7 vectors, respectively. Following sequencing, the recombinant segment of the correct clone was incised by BamHI and XbaI (Takara). The recombinant segment was inserted into pMSCV-hygro, which was incised by the same two restriction endonucleases. The clones were sequenced, and the correct clones were amplified and identified before transfection into H9c2 cells.

ELISA for Soluble Inflammatory Cytokines

The expression levels of inflammatory factors IL-6, IL-1 β , and TNF- α in cell supernatants or serum were measured using commercially available ELISA kits (Elabscience Biotechnology, Wuhan, China). In accordance with the manufacturer's instructions, supernatants were stored at -80°C before measurements, and both standards and samples were run in triplicate. The optical density (OD)₄₅₀ was calculated by subtracting the background, and standard curves were plotted.

MI Model

MI was produced by surgical ligation of the left anterior descending coronary artery (LAD). After animals were anesthetized with keta-

mine hydrochloride (50 mg/kg) and diazepam (5 mg/kg), the chest was opened at the left fourth intercostal space, and the LAD was ligated with a 6-0 silk suture 1 mm below the tip of the left atrial appendage. Successful ligation was verified by color change. To analyze the effect of exosomes on myocardial tissue, we suspended exosomes (400 μg of protein) from different groups in 200 μL of PBS and administered them by intravenous injection immediately after the ligation operation. Animals were then followed for 1 additional month and then euthanized. Cardiac muscle tissues were collected for histochemical analyses.

Measurement of Infarct Volume

Measurement of infarct volumes was performed as previously described.⁴⁴ In brief, the heart was harvested and rinsed with normal saline. The excised left ventricle was frozen at -20°C for 30 min and then sectioned from apex to base into ~ 2 -mm slices. The slices were incubated in a solution of 1% TTC in PBS (pH 7.4) at 37°C for 15 min in darkness and then fixed in 10% formaldehyde. The slices were photographed the next day using a digital camera. The infarcted (non-TTC-stained) area was isolated from the rest of the cardiac tissue, which was stained red by TTC. The infarct size was expressed as a percentage of the mass of the left ventricle.

Immunohistochemistry

To measure apoptosis, we fixed and labeled cardiomyocytes or myocardial tissues using TUNEL using a commercially available kit (*In Situ* Cell Death Detection Kit; Roche Diagnostics, Basel, Switzerland) to label the apoptotic cell nuclei. To identify myocardial tissue damage, we stained myocardial tissues with H&E. Sections were examined with an Axiophot light microscope (Zeiss, Oberkochen, Germany) and photographed with a digital camera.

Luciferase Reporter Assay

To investigate whether miR-93-5p directly regulated TLR4 and Atg7 expression, we inserted the sequences of the 3' UTR of TLR4 and Atg7 downstream of a Renilla luciferase open reading frame in the pGL3-CMV vector (Promega, Madison, WI, USA). HEK293T cells were transfected with the pGL3-basic construct along with either the miR-93-5p mimic or a scrambled control using Lipofectamine 2000 (Invitrogen). After 48 hr, the cells were harvested, and luciferase activity was measured. Results are presented as the ratio of Renilla luciferase activity to firefly luciferase activity. All of these experiments were performed at Yingbai Corporation (Shanghai, China).

Figure 6. miR-93-5p Expression in H9c2 Cells Showed that Hypoxia Induced Myocardial Cell Injury by Suppressing Atg7-Mediated Autophagy

H9c2 cells were transfected with miR-93-5p mimic and/or Atg7 overexpression vector for 48 hr before exposure to hypoxic conditions for 24 hr; then cells were collected for subsequent experiments. (A) RT-PCR shows the expression of miR-93-5p in H9c2 cells after transfection with miR-93-5p mimic for 48 hr. The data are presented as mean \pm SD (n = 3). ***p < 0.001 versus control group. (B and C) Western blotting (B) and RT-PCR (C) showed the expression of Atg7 in H9c2 cells after transfection with Atg7 overexpression vector for 48 hr. The data are presented as mean \pm SD (n = 3). ***p < 0.001 versus control group. (D) Apoptosis of H9c2 cells was assessed using flow cytometry with AV-FITC staining. (E) The relative apoptosis ratio was analyzed at least five times. Data are presented as the mean \pm SD. n = 5. ***p < 0.001 versus control group; ###p < 0.001 versus hypoxia group. (F) Immunofluorescence showed autophagy plaques in H9c2 cells transiently expressing GFP-LC3 after different treatments. Scale bars, 20 μm . (G) The number of GFP-LC3 dots was counted in 10 independent visual fields. Data are presented as the mean \pm SD. n = 10. ***p < 0.001 versus control group; ###p < 0.001 versus hypoxia group. (H) The expression of LC3 and P62 in H9c2 cells was measured with western blotting. (I) Protein expression was quantified. (J) The data are presented as means \pm SD. n = 3. ***p < 0.001 versus control; ####p < 0.001 versus hypoxia group.

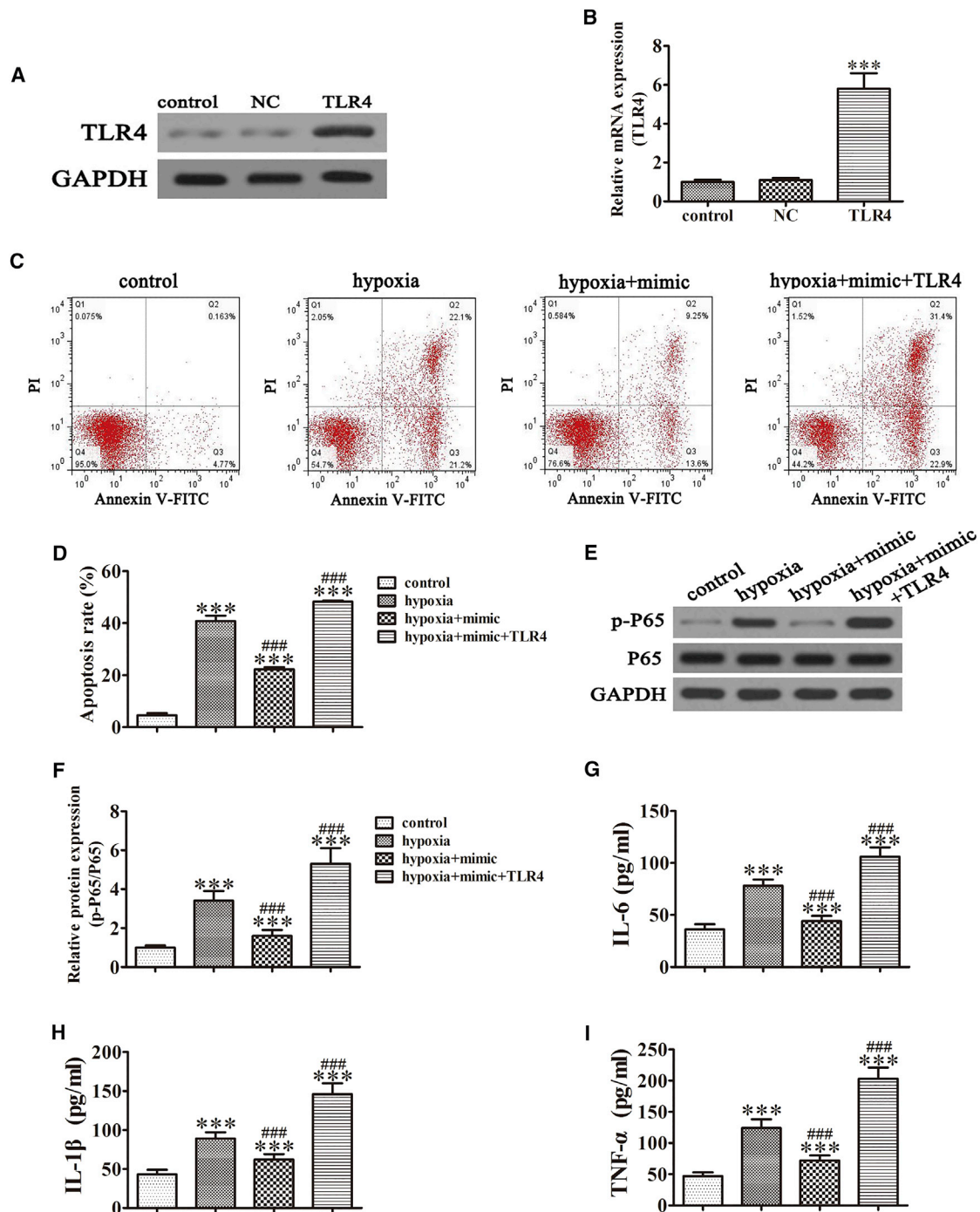


Figure 7. The Expression of miR-93-5p in H9c2 Cells Inhibited Hypoxia-Induced Myocardial Cell Injury by Suppressing the TLR4/NF- κ B-Mediated Inflammatory Response

H9c2 cells transfected with miR-93-5p mimic and/or TLR4 overexpression vector for 48 hr before exposure to hypoxic conditions for 24 hr. Then H9c2 cells were collected for subsequent experiments. (A and B) Western blotting (A) and RT-PCR (B) showed the expression of TLR4 in H9c2 cells after transfection with TLR4 overexpression vector for 48 hr. The data are presented as mean \pm SD (n = 3). ***p < 0.001 versus control group. (C) Apoptosis of H9c2 cells was assessed using flow cytometry with Annexin V-FITC staining. (D) The relative apoptosis ratio was analyzed at least five times. Data are presented as the mean \pm SD. n = 5. ***p < 0.001 versus normal group; ###p < 0.001 versus hypoxia group. (E) Western blotting showed the expression of NF- κ B. (F) Protein expression was quantified. The data are presented as means \pm SD. ***p < 0.001 versus control; ###p < 0.001 versus hypoxia group. (G-I) ELISA showed the expression of the inflammatory factors IL-6 (G), IL-1 β (H), and TNF- α (I) in cellular supernatant. Data are presented as means \pm SD. ***p < 0.001 versus control; ###p < 0.001 versus hypoxia group.

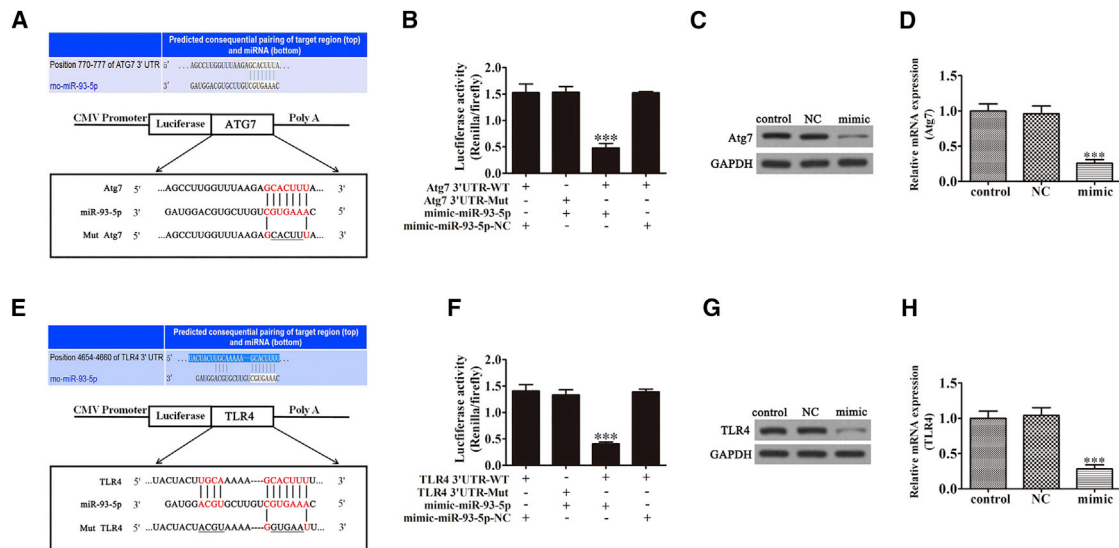


Figure 8. Both Atg7 and TLR4 Were Direct Targets of miR-93-5p

(A) Complementary sequences between miR-93-5p and the 3' UTR of Atg7 mRNA were obtained using publicly available algorithms. The mutated version of the Atg7 3' UTR is also shown. (B) The 3' UTR of Atg7 was fused to the luciferase coding region (PYr-Atg7 3' UTR) and co-transfected into HEK293T cells with miR-93-5p mimic to confirm that Atg7 is the target of miR-93-5p. The PYr-RGS-17 3' UTR and miR-93-5p mimic constructs were co-transfected into HEK293T cells with a control vector, and the relative luciferase activity was determined 48 hr after transfection. Data are expressed as the mean \pm SD. (C and D) Western blotting (C) and RT-PCR (D) analysis of Atg7 expression in H9c2 cells after transfection with miR-93-5p mimic (n = 3). GAPDH expression levels were measured as an endogenous control. The data are expressed as the mean \pm SD. (E) Complementary sequences between miR-93-5p and the 3' UTR of TLR4. The mutated version of the TLR4 3' UTR is also shown. (F) The 3' UTR of TLR4 was fused to the luciferase coding region (PYr-TLR4 3' UTR) and co-transfected into HEK293T cells with miR-93-5p mimic to confirm that TLR4 is the target of miR-93-5p. The PYr-RGS-17 3' UTR and miR-93-5p mimic constructs were co-transfected into HEK293T cells with a control vector, and the relative luciferase activity was determined 48 hr after transfection. The data are expressed as mean \pm SD. (G and H) Western blotting (G) and RT-PCR (H) analysis of TLR4 expression in H9c2 cells after transfection with miR-93-5p mimic (n = 3). GAPDH expression levels were measured as an endogenous control. The data are expressed as mean \pm SD. ***p < 0.001 versus control.

Western Blot Analysis

Western blotting was performed as previously described.⁴⁵ After nonspecific binding was blocked, the membranes were incubated with primary antibodies against P65 (1:200), p-P65 (1:500), P62 (1:500), LC3 (1:200), Atg7 (1:200), TLR4 (1:500), and GAPDH (1:1,000) (Sigma-Aldrich, St. Louis, MO, USA). Immunoreactive proteins were visualized using enhanced chemiluminescence detection (Bioworld Technology, Nanjing, China). Immunoreactive labeling was analyzed with ImageJ 1.44 and normalized to GAPDH protein levels.

Statistical Analysis

Results are expressed as the mean \pm SD. Statistical significance was evaluated by ANOVA followed by Tukey-Kramer multiple comparison test and by Student's t test. p < 0.05 denotes statistical significance.

AUTHOR CONTRIBUTIONS

H.W., M. Jiang, J.L., H.H., and Y.Z. generated and analyzed data. J.L., M. Jin, S.D., H.R., X.S., and P.G. designed experiments and drafted the manuscript.

CONFLICTS OF INTEREST

The authors declare that there is no conflict of interest.

ACKNOWLEDGMENTS

This study was supported by the Featured Special Disease Fund of Pudong New District (grant PWZzb2017-27 to H.W.), the Science and Technology Development Fund of Pudong New District Minsheng Scientific Research (Medical and Health) Project (grant PKJ2017-Y24 to M. Jiang), the Foundation of Discipline Leader in Health Systems of Pudong New District (grant PWRd2011-04 to H.W., grant PWRd2014-09 to M. Jiang), and the National Natural Science Foundation of China (grant 81700428 to S.D.).

REFERENCES

- Yang, W.J., Yang, D.D., Na, S., Sandusky, G.E., Zhang, Q., and Zhao, G. (2005). Dicer is required for embryonic angiogenesis during mouse development. *J. Biol. Chem.* 280, 9330–9335.
- Amado, L.C., Saliaris, A.P., Schuleri, K.H., St John, M., Xie, J.S., Cattaneo, S., Durand, D.J., Fitton, T., Kuang, J.Q., Stewart, G., et al. (2005). Cardiac repair with intramyocardial injection of allogeneic mesenchymal stem cells after myocardial infarction. *Proc. Natl. Acad. Sci. USA* 102, 11474–11479.
- Schuleri, K.H., Feigenbaum, G.S., Centola, M., Weiss, E.S., Zimmet, J.M., Turney, J., Kellner, J., Zviman, M.M., Hatzistergos, K.E., Detrick, B., et al. (2009). Autologous mesenchymal stem cells produce reverse remodeling in chronic ischaemic cardiomyopathy. *Eur. Heart J.* 30, 2722–2732.
- Hare, J.M., Fishman, J.E., Gerstenblith, G., DiFede Velazquez, D.L., Zambrano, J.P., Suncion, V.Y., Tracy, M., Ghersin, E., Johnston, P.V., Brinker, J.A., et al. (2012). Comparison of allogeneic vs autologous bone marrow-derived mesenchymal stem

- cells delivered by transcatheter injection in patients with ischemic cardiomyopathy: the POSEIDON randomized trial. *JAMA* 308, 2369–2379.
5. Lee, J.W., Lee, S.H., Youn, Y.J., Ahn, M.S., Kim, J.Y., Yoo, B.S., Yoon, J., Kwon, W., Hong, I.S., Lee, K., et al. (2014). A randomized, open-label, multicenter trial for the safety and efficacy of adult mesenchymal stem cells after acute myocardial infarction. *J. Korean Med. Sci.* 29, 23–31.
 6. Otto Beitnes, J., Oie, E., Shahdadfar, A., Karlsen, T., Müller, R.M., Aakhus, S., Reinhold, F.P., and Brinchmann, J.E. (2012). Intramyocardial injections of human mesenchymal stem cells following acute myocardial infarction modulate scar formation and improve left ventricular function. *Cell Transplant.* 21, 1697–1709.
 7. Kim, J.H., Joo, H.J., Kim, M., Choi, S.C., Lee, J.I., Hong, S.J., and Lim, D.S. (2017). Transplantation of adipose-derived stem cell sheet attenuates adverse cardiac remodeling in acute myocardial infarction. *Tissue Eng. Part A* 23, 1–11.
 8. Toma, C., Pittenger, M.F., Cahill, K.S., Byrne, B.J., and Kessler, P.D. (2002). Human mesenchymal stem cells differentiate to a cardiomyocyte phenotype in the adult murine heart. *Circulation* 105, 93–98.
 9. Freyman, T., Polin, G., Osman, H., Crary, J., Lu, M., Cheng, L., Palasis, M., and Wilensky, R.L. (2006). A quantitative, randomized study evaluating three methods of mesenchymal stem cell delivery following myocardial infarction. *Eur. Heart J.* 27, 1114–1122.
 10. Fischer, U.M., Harting, M.T., Jimenez, F., Monzon-Posadas, W.O., Xue, H., Savitz, S.I., Laine, G.A., and Cox, C.S., Jr. (2009). Pulmonary passage is a major obstacle for intravenous stem cell delivery: the pulmonary first-pass effect. *Stem Cells Dev.* 18, 683–692.
 11. Gnecci, M., He, H., Noiseux, N., Liang, O.D., Zhang, L., Morello, F., Mu, H., Melo, L.G., Pratt, R.E., Ingwall, J.S., and Dzau, V.J. (2006). Evidence supporting paracrine hypothesis for Akt-modified mesenchymal stem cell-mediated cardiac protection and functional improvement. *FASEB J.* 20, 661–669.
 12. Mirosou, M., Zhang, Z., Deb, A., Zhang, L., Gnecci, M., Noiseux, N., Mu, H., Pachori, A., and Dzau, V. (2007). Secreted frizzled related protein 2 (Sfrp2) is the key Akt-mesenchymal stem cell-released paracrine factor mediating myocardial survival and repair. *Proc. Natl. Acad. Sci. USA* 104, 1643–1648.
 13. Jeong, J.O., Han, J.W., Kim, J.M., Cho, H.J., Park, C., Lee, N., Kim, D.W., and Yoon, Y.S. (2011). Malignant tumor formation after transplantation of short-term cultured bone marrow mesenchymal stem cells in experimental myocardial infarction and diabetic neuropathy. *Circ. Res.* 108, 1340–1347.
 14. Ailawadi, S., Wang, X., Gu, H., and Fan, G.C. (2015). Pathologic function and therapeutic potential of exosomes in cardiovascular disease. *Biochim. Biophys. Acta* 1852, 1–11.
 15. Yuan, M., Zhang, L., You, F., Zhou, J., Ma, Y., Yang, F., and Tao, L. (2017). MiR-145-5p regulates hypoxia-induced inflammatory response and apoptosis in cardiomyocytes by targeting CD40. *Mol. Cell. Biochem.* 431, 123–131.
 16. Zhang, Y., Cheng, J., Chen, F., Wu, C., Zhang, J., Ren, X., Pan, Y., Nie, B., Li, Q., and Li, Y. (2017). Circulating endothelial microparticles and miR-92a in acute myocardial infarction. *Biosci. Rep.* 37, BSR20170047.
 17. Li, K., Lin, T., Chen, L., and Wang, N. (2017). MicroRNA-93 elevation after myocardial infarction is cardiac protective. *Med. Hypotheses* 106, 23–25.
 18. Fabbri, E., Montagner, G., Bianchi, N., Finotti, A., Borgatti, M., Lampronti, I., Cabrini, G., and Gambari, R. (2016). MicroRNA miR-93-5p regulates expression of IL-8 and VEGF in neuroblastoma SK-N-AS cells. *Oncol. Rep.* 35, 2866–2872.
 19. Chen, S.M., Wang, B.Y., Lee, C.H., Lee, H.T., Li, J.J., Hong, G.C., Hung, Y.C., Chien, P.J., Chang, C.Y., Hsu, L.S., and Chang, W.W. (2017). Hinokitol up-regulates miR-494-3p to suppress BMI1 expression and inhibits self-renewal of breast cancer stem/progenitor cells. *Oncotarget* 8, 76057–76068.
 20. Wang, Z., Yuan, B., Fu, F., Huang, S., and Yang, Z. (2017). Hemoglobin enhances miRNA-144 expression and autophagic activation mediated inflammation of microglia via mTOR pathway. *Sci. Rep.* 7, 11861.
 21. de Castro, A.L., Fernandes, R.O., Ortiz, V.D., Campos, C., Bonetto, J.H.P., Fernandes, T.R.G., Conzatti, A., Siqueira, R., Tavares, A.V., Belló-Klein, A., and da Rosa Araujo, A.S. (2018). Thyroid hormones decrease the proinflammatory TLR4/NF- κ B pathway and improve functional parameters of the left ventricle of infarcted rats. *Mol. Cell. Endocrinol.* 416, 132–142.
 22. Wu, X., Zheng, D., Qin, Y., Liu, Z., Zhang, G., Zhu, X., Zeng, L., and Liang, Z. (2017). Nobiletin attenuates adverse cardiac remodeling after acute myocardial infarction in rats via restoring autophagy flux. *Biochem. Biophys. Res. Commun.* 492, 262–268.
 23. Zhang, Z., Li, H., Chen, S., Li, Y., Cui, Z., and Ma, J. (2017). Knockdown of microRNA-122 protects H9c2 cardiomyocytes from hypoxia-induced apoptosis and promotes autophagy. *Med. Sci. Monit.* 23, 4284–4290.
 24. Liang, Y., Zhou, T., Chen, Y., Lin, D., Jing, X., Peng, S., Zheng, D., Zeng, Z., Lei, M., Wu, X., et al. (2017). Rifampicin inhibits rotenone-induced microglial inflammation via enhancement of autophagy. *Neurotoxicology* 63, 137–145.
 25. Li, H., Zhang, Y., Min, J., Gao, L., Zhang, R., and Yang, Y. (2018). Astragaloside IV attenuates orbital inflammation in Graves' orbitopathy through suppression of autophagy. *Inflamm. Res.* 67, 117–127.
 26. Qu, Y., Zhang, Q., Cai, X., Li, F., Ma, Z., Xu, M., and Lu, L. (2017). Exosomes derived from miR-181-5p-modified adipose-derived mesenchymal stem cells prevent liver fibrosis via autophagy activation. *J. Cell. Mol. Med.* 21, 2491–2502.
 27. Chen, F., Zhang, H., Wang, Z., Ding, W., Zeng, Q., Liu, W., Huang, C., He, S., and Wei, A. (2017). Adipose-derived stem cell-derived exosomes ameliorate erectile dysfunction in a rat model of type 2 diabetes. *J. Sex. Med.* 14, 1084–1094.
 28. Pu, C.M., Liu, C.W., Liang, C.J., Yen, Y.H., Chen, S.H., Jiang-Shieh, Y.F., Chien, C.L., Chen, Y.C., and Chen, Y.L. (2017). Adipose-derived stem cells protect skin flaps against ischemia/reperfusion injury via IL-6 expression. *J. Invest. Dermatol.* 137, 1353–1362.
 29. Long, G., Wang, F., Duan, Q., Yang, S., Chen, F., Gong, W., Yang, X., Wang, Y., Chen, C., and Wang, D.W. (2012). Circulating miR-30a, miR-195 and let-7b associated with acute myocardial infarction. *PLoS ONE* 7, e50926.
 30. Desrochers, L.M., Antonyak, M.A., and Cerione, R.A. (2016). Extracellular vesicles: satellites of information transfer in cancer and stem cell biology. *Dev. Cell* 37, 301–309.
 31. Pitt, J.M., Kroemer, G., and Zitvogel, L. (2016). Extracellular vesicles: masters of intercellular communication and potential clinical interventions. *J. Clin. Invest.* 126, 1139–1143.
 32. Sato, K., Meng, F., Glaser, S., and Alpini, G. (2016). Exosomes in liver pathology. *J. Hepatol.* 65, 213–221.
 33. Suzuki, E., Fujita, D., Takahashi, M., Oba, S., and Nishimatsu, H. (2017). Therapeutic effects of mesenchymal stem cell-derived exosomes in cardiovascular disease. *Adv. Exp. Med. Biol.* 998, 179–185.
 34. Zhao, Y., Sun, X., Cao, W., Ma, J., Sun, L., Qian, H., Zhu, W., and Xu, W. (2015). Exosomes derived from human umbilical cord mesenchymal stem cells relieve acute myocardial ischemic injury. *Stem Cells Int.* 2015, 761643.
 35. Gallet, R., Dawkins, J., Valle, J., Simsolo, E., de Couto, G., Middleton, R., Tseliou, E., Luthringer, D., Kreke, M., Smith, R.R., et al. (2017). Exosomes secreted by cardiomyocytes reduce scarring, attenuate adverse remodeling, and improve function in acute and chronic porcine myocardial infarction. *Eur. Heart J.* 38, 201–211.
 36. Phinney, D.G., Di Giuseppe, M., Njah, J., Sala, E., Shiva, S., St Croix, C.M., Stolz, D.B., Watkins, S.C., Di, Y.P., Leikauf, G.D., et al. (2015). Mesenchymal stem cells use extracellular vesicles to outsource mitophagy and shuttle microRNAs. *Nat. Commun.* 6, 8472.
 37. Katakowski, M., Buller, B., Zheng, X., Lu, Y., Rogers, T., Osobamiro, O., Shu, W., Jiang, F., and Chopp, M. (2013). Exosomes from marrow stromal cells expressing miR-146b inhibit glioma growth. *Cancer Lett.* 335, 201–204.
 38. Bhutia, S.K., Kegelman, T.P., Das, S.K., Azab, B., Su, Z.Z., Lee, S.G., Sarkar, D., and Fisher, P.B. (2010). Astrocyte elevated gene-1 induces protective autophagy. *Proc. Natl. Acad. Sci. USA* 107, 22243–22248.
 39. Ouyang, L., Shi, Z., Zhao, S., Wang, F.T., Zhou, T.T., Liu, B., and Bao, J.K. (2012). Programmed cell death pathways in cancer: a review of apoptosis, autophagy and programmed necrosis. *Cell Prolif.* 45, 487–498.
 40. Kashiwagi, M., Imanishi, T., Ozaki, Y., Satogami, K., Masuno, T., Wada, T., Nakatani, Y., Ishibashi, K., Komukai, K., Tanimoto, T., et al. (2012). Differential expression of Toll-like receptor 4 and human monocyte subsets in acute myocardial infarction. *Atherosclerosis* 221, 249–253.

41. Džumhur, A., Zibar, L., Wagner, J., Simundić, T., Dembić, Z., and Barbić, J. (2012). Association studies of gene polymorphisms in toll-like receptors 2 and 4 in Croatian patients with acute myocardial infarction. *Scand. J. Immunol.* *75*, 517–523.
42. Ding, H.S., Yang, J., Chen, P., Yang, J., Bo, S.Q., Ding, J.W., and Yu, Q.Q. (2013). The HMGB1-TLR4 axis contributes to myocardial ischemia/reperfusion injury via regulation of cardiomyocyte apoptosis. *Gene* *527*, 389–393.
43. Chen, X., Yan, L., Guo, Z., Chen, Z., Chen, Y., Li, M., Huang, C., Zhang, X., and Chen, L. (2016). Adipose-derived mesenchymal stem cells promote the survival of fat grafts via crosstalk between the Nrf2 and TLR4 pathways. *Cell Death Dis.* *7*, e2369.
44. Yao, C., Shi, X., Lin, X., Shen, L., Xu, D., and Feng, Y. (2015). Increased cardiac distribution of mono-PEGylated Radix Ophiopogonis polysaccharide in both myocardial infarction and ischemia/reperfusion rats. *Int. J. Nanomedicine* *10*, 409–418.
45. Suzuki, A., Hanada, T., Mitsuyama, K., Yoshida, T., Kamizono, S., Hoshino, T., Kubo, M., Yamashita, A., Okabe, M., Takeda, K., et al. (2001). CIS3/SOCS3/SSI3 plays a negative regulatory role in STAT3 activation and intestinal inflammation. *J. Exp. Med.* *193*, 471–481.